INTERNATIONAL SOCIETY FOR
SOIL MECHANICS AND
GEOTECHNICAL ENGINEERING

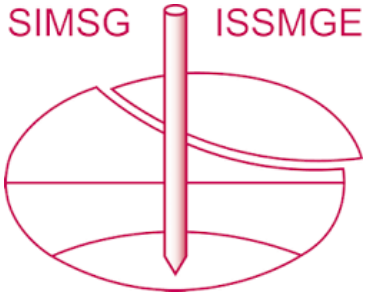

This paper was downloaded from the Online Library of the International Society for Soil Mechanics and Geotechnical Engineering (ISSMGE). The library is available here:

https://www.issmge.org/publications/online-library

This is an open-access database that archives thousands of papers published under the Auspices of the ISSMGE and maintained by the Innovation and Development Committee of ISSMGE.

The paper was published in the proceedings of the 7th International Conference on Earthquake Geotechnical Engineering and was edited by Francesco Silvestri, Nicola Moraci and Susanna Antonielli. The conference was held in Rome, Italy, 17 – 20 June 2019.

Earthquake Geotechnical Engineering for Protection and Development of Environment and Constructions – Silvestri & Moraci (Eds)
© 2019 Associazione Geotecnica Italiana, Rome, Italy, ISBN 978-0-367-14328-2

Vulnerability assessment for masonry buildings based on observed damage from the 2016 Amatrice Earthquake

A. Miano, F. Jalayer, G. Forte & A. Santo
University of Naples Federico II, Italy

ABSTRACT: Recent earthquakes around the world and in Italy showed the seismic vulnerability of the existing building stock. This evidence stresses the need to develop accurate seismic fragili-ty tools, to be applied at territorial scale. Herein, seismic vulnerability curves for existing masonry buildings are developed, based on damage assessment carried out through visual survey and the Copernicus damage maps using EMS-98 damage scale. The observed dam-age dataset consists of damages occurred due to the 24th August 2016 Amatrice earthquake. The study focuses on seven towns close to the epicentre of Amatrice earthquake. The masonry building stock consists of selected buildings belonging to these towns. Ac-celerometric registrations for the considered earthquake are used to update the GMPE pre-dictions. The resulting ground shaking fields have been modified through application of explicit stratigraphic and topographic factors. It has been confirmed that explicit consider-ation of local site effects can significantly affect the seismic vulnerability evaluations.

1 INTRODUCTION

Assessment of seismic risk for buildings at a territorial scale depends to a large extent on the availability of reliable and reasonably accurate fragility curves. The seismic fragility curves can be classified into four categories (Rossetto and Elnashai 2003); namely, 1) analytic (e.g., Baker 2015, Jalayer et al. 2017, Miano et al. 2018), 2) empirical, 3) based on expert opinion, and 4) hybrid (e.g., Singhal and Kiremidjian 1998). The empirical fragility curves can provide a realistic picture of post-earthquake damage. The shortcomings related to empirical fragility assessment are mainly associated to the difficulties in creating a homogenous class of buildings, inaccurate estimation of seismic ground shaking, site effects and the observed damage (Crawley et al. 2008, Lallemant et al. 2015). One essential requirement for derivation of useful empirical fragility curves is to refer to a standardized damage scale. The European Microseismic Scale (EMS-98, Grünthal, 1998) is often used to report the empirical fragility curves in Europe. Several works have focused on empirical assessment of the vulnerability of Italian building stock (mainly masonry and reinforced concrete). With respect to Italian masonry buildings, typically low- to mid-rise, Lagomarsino and Giovinazzi (2006) have derived vulnerability curves reporting the mean damage ratio versus seismic intensity expressed in the EMS-98 scale. Zuccaro and Cacace (2015) proposed a methodology to reduce the variability in the vulnerability classification of EMS-98 through the application of vulnerability modifiers. Rota et al. 2008 derived empirical fragility curves based on damage survey data for 150,000 buildings from past Italian earthquakes, occurred in the period spanning from Irpinia (1980) to Molise (2002) earthquakes. It is to note that this work follows the masonry buildings classes definition presented in Rota et al. 2008. De Luca et al. (2015) derived empirical fragility curves based on a database of 131 post-earthquake building surveys conducted on RC buildings located in Pettino town after the 2009 L'Aquila Earthquake. Del Gaudio et al. (2017) have derived empirical fragility curves based on the large database of post L'Aquila Earthquake (2009) damage survey conducted by the Italian Civil Protection (Dolce and Goretti 2015) on RC buildings.

This work presents a methodology for the generation of conditional GMPE-based percentiles (i.e., median, 16^{th} and 84^{th}) of ground shaking fields for derivation of empirical fragility curves. The fragility curves are defined as the probability of exceeding a specific damage state given a certain level of PGA. The application of this methodology is demonstrated in deriving empirical fragility curves based on damage data for masonry buildings after the 2016 Amatrice Earthquake. The basic underlying idea is similar to the method described in Park et al. 2007, Miano et al. 2015 and 2016 for portfolio loss assessment and consists of the following tasks, obtained using the software MATLAB (MATLAB 2016b): (a) The ground shaking propagated to the bed rock level using the GMPE is modified (or propagated to the surface) based on site-specific stratigraphic and topographic factors (coefficients to be multiplied to the acceleration at the bed rock); (b) a complete GMPE representation through the joint Lognormal probability distribution is updated based on the recorded registrations of the earthquake event of interest at the surrounding stations; (c) the structural vulnerability curve for a designated class is developed based on the ground-shaking percentiles estimated at the site of each building and the corresponding observed damage level.

2 METHODOLOGY

The joint probability density function $f(\mathbf{PGA})$ for the vector of $\mathbf{PGA}=[PGA_i,\ i=1{:}N_{cl}]$ values at the location of N_{cl} buildings of interest belonging to a specific class CL (see Chapter 3 for the classes definition), for a given earthquake scenario, can be evaluated by employing a ground motion prediction equation (GMPE). Assuming that the PGA values at the location of each surveyed building are distributed as a joint multi-variate (log) Normal distribution, a full probabilistic representation of GMPE, which is identified by its expected value vector $\mathbf{M}$ and covariance matrix $\mathbf{\Sigma}$, can be constructed. Once the first two moments are known, several realizations of the ground shaking field can be generated and their median can be calculated. Referring to the GMPE developed by Bindi et al. (2011) for the peak ground acceleration (PGA, the geometric mean of two horizontal components) and based on a collection of Italian seismic events, the median predicted PGA can be written as:

$$\mathrm{E}[\log_{10}\mathrm{PGA}] = e_1 + F_D\left(R_{jb}, M\right) + F_M(M) + F_S + F_{sof} \tag{1}$$

where $\mathrm{E}[\log_{10}\mathrm{PGA}]$ is the expected value (first moment) for the (base 10) logarithm of peak ground acceleration (PGA, in $\mathrm{cm/s^2}$); e_1 is a constant term, F_D (R_{jb},M), $F_M(M)$, F_s and F_{sof} represent the distance function, the magnitude scaling, the site amplification and the style of faulting correction, respectively. M is the moment magnitude (generally referred as M_w), R_{jb} is the Joyner–Boore distance in km. The values $\mathrm{E}[\log_{10}\mathrm{PGA_i}]$ ($i=1{:}N_{cl}$) from Eq. 1 constitute the components of the mean vector $\mathbf{M}$ for N_{cl} buildings belonging to a specific class CL. The covariance matrix, $\mathbf{\Sigma}$, is defined as the sum of two inter-event and intra-event components:

$$\mathbf{\Sigma} = \sigma^2_{INTER} \cdot \mathrm{e} + \sigma^2_{INTRA} \cdot \mathrm{R} \tag{2}$$

where σ_{intra} represents the intra-event variability and σ_{inter} represents the inter-event variability (both parameters are tabulated in Bindi et al. 2011); $\mathbf{e}$ is the all ones matrix and $\mathbf{R}$ is the matrix of correlation coefficients. $\mathbf{R}$ is composed of unit diagonal terms and off-diagonals equal to ρ_{jk}, $j\neq k$ (varying from 1 to N_{cl}). The covariance matrix is obtained according to the formulation of ρ_{jk} from Esposito and Iervolino, 2012:

$$\rho_{jk} = \exp\left[-3 \cdot h_{jk}/b(T)\right] \tag{3}$$

where h_{jk} is the distance between sites j and k and $b(T)$ is a coefficient equal to 10.8km. The GMPE adopted herein (Bindi et al. 2011) considers the site effects as a function of V_{s30}-dependent European Code soil classifications. Nevertheless, it is important to incorporate the results of more sophisticated seismic microzonation studies or soil class map (i.e. Forte et al., 2017) for the surveyed buildings sites. For example, Landolfi et al. (2011) and later Tropeano

et al. (2018) propose site-specific stratigraphic coefficients that consider non-linear soil column propagation effects. Two alternatives are considered for taking into account the stratigraphic site effect; namely, (a) the coefficients imbedded in the GMPE (here Bindi et al. 2011); (b) application of stratigraphic amplification factors, that consider non-linear soil column propagation effects, to ground shaking fields propagated to bedrock (e.g., those reported in Landolfi et al. 2011). In option (b), the site effects are evaluated through the stratigraphic amplification factor, directly multiplied by the reference (i.e., propagated to bed-rock) peak ground acceleration from the GMPE by Bindi et al. (2011) to obtain the peak acceleration at surface. In a similar manner, it is also possible to apply topographic factors (S_T) to the GMPE (directly multiplying S_T to the reference PGA from GMPE). S_T depends on the shape of slopes; since irregular surface geometry affects the focusing, defocusing, diffraction and scattering of seismic waves. A geometrical parameter more suitable for small scale studies is the slope curvature, which can be obtained from the Digital Elevation Model (DEM) of the area. This index permits to mark the concave and the convex features of a landscape, with negative and positive values accounting for attenuation in valleys and the seismic waves focusing on ridges. The effectiveness of this parameter was also validated by the numerical study of Torgoev et al. (2013) and adopted in seismic slope stability analyses by Silvestri et al. (2016). One interesting feature of the joint Normal distribution attributed herein to the PGA values at the buildings' sites for a specific class is that the distribution parameters can be updated based on the registered accelerometric values. Let the vector of mean values $\mathbf{M}$ and the covariance matrix $\mathbf{\Sigma}$ be partitioned as follows (Park et al. 2007):

$$\mathbf{M} = \begin{bmatrix} \mathbf{M}_1 \\ \mathbf{M}_2 \end{bmatrix} \qquad \mathbf{\Sigma} = \begin{bmatrix} \mathbf{\Sigma}_{11} & \mathbf{\Sigma}_{12} \\ \mathbf{\Sigma}_{21} & \mathbf{\Sigma}_{22} \end{bmatrix} \tag{4}$$

where $\mathbf{M_1}$ is the mean (of the base 10 logarithm) vector of $\mathbf{PGA}=[PGA_i,\ i=1{:}N_{cl}]$ values according to the adopted GMPE; $\mathbf{M_2}$ is the mean vector of calculated $\log_{10}$PGA at the stations within the area of interest (according to the adopted GMPE); $\mathbf{\Sigma_{11}}$ is the covariance matrix for the calculated (from the GMPE) $\log_{10}$PGA for the surveyed buildings of class *CL*; $\mathbf{\Sigma_{12}}=\mathbf{\Sigma_{21}}$ is the cross-covariance matrix for the $\log_{10}$PGA values calculated (from the GMPE) at the location of the surveyed buildings and those calculated at the location of the stations; $\mathbf{\Sigma_{22}}$ is the covariance matrix for the $\log_{10}$PGA values calculated at the stations. The conditional distribution of the calculated $\log_{10}$PGA values given the registered $\log_{10}$PGA values at the stations is also a joint Normal distribution with mean vector $\mathbf{M_{1|2}}$ and covariance matrix $\mathbf{\Sigma_{11|22}}$:

$$\mathbf{M_{1|2}} = \mathbf{M_1} + \mathbf{\Sigma}_{12} \cdot \mathbf{\Sigma}_{22}^{-1} \cdot (x_2 - \mathbf{M_2}); \mathbf{\Sigma}_{11|22} = \mathbf{\Sigma}_{11} - \mathbf{\Sigma}_{12} \cdot \mathbf{\Sigma}_{22}^{-1} \cdot \mathbf{\Sigma}_{21} \tag{5}$$

where x_2 is the vector of the registered $\log_{10}$PGA values for the stations.

The empirical vulnerability curves have been calculated according to a logistic regression probability model (see e.g. Charvet et al. 2014, Jalayer and Ebrahimian 2017, De Risi et al. 2017). This type of regression is suitable for cases where the dependent variable is binary (i.e., either 0 or 1). Thus, it is especially suitable for estimating the probability of exceeding a damage state D_i. The vulnerability curves for each designated building class, $P(D>D_i|PGA^{p\%})$, have been calculated based on data pairs containing the 16th percentile (p=0.16), median (p=0.50), and 84th (p=0.84) percentiles of the ground shaking in terms of PGA evaluated through the updated GMPE (i.e., with statistics updated through Eq. 5 expressions) versus observed damage (based on EMS-98) for the buildings of each class. It is to note that using the percentiles of the ground-shaking at each location implies that the spatial correlation and the uncertainty in ground-shaking is not going to be explicitly considered in deriving the seismic vulnerability curves. The vulnerability curves $P(D>D_i|PGA^{p\%})$ derived are not suitable for integration with seismic hazard as they are shown in term of PGA percentiles as opposed to the PGA values registered at a given location (hence the use of term "vulnerability" instead of "fragility").

3 CASE STUDY: MASONRY BUILDINGS DAMAGED BY AMATRICE EARTHQUAKE

Between August and October 2016, Central Italy was stricken by three damaging earthquakes. The vulnerability study carried out in this paper refers to the first event, with Mw 6.0 event and occurred on August 24th at 01:36 UTC close to Accumoli village (herein referred to as Amatrice Earthquake, see Ebrahimian and Jalayer 2018 for more details about the Central Italy seismic sequence). The European Macroseismic Scale EMS 1998 (Grünthal 1998) classification is used herein in order to identify the damage to the portfolio of masonry buildings considered. The grades of damage are described as follows: **Grade 1 (D_1):** Negligible to slight damage. There is no structural damage and slight non-structural damage; **Grade 2 (D_2):** Moderate damage. There is slight structural damage and moderate non-structural damage; **Grade 3 (D_3):** Substantial to heavy damage. There is moderate structural damage and heavy non-structural damage; **Grade 4 (D_4):** Very heavy damage; **Grade 5 (D_5):** Destruction. Identification of the damage level for different buildings has been carried out through two alternative surveying techniques; namely satellite imagery through Copernicus-EMS damage grading and visual survey. The observed damage dataset is related to the 24th August 2016 Amatrice earthquake and the aftershocks that immediately succeed it. The Copernicus (Copernicus 2016) EMS provides rapid assessment of the damages through generation of "damage grading" maps, made possible by comparing pre- and post-event satellite images. It turns out that satellite imagery is more reliable for damage grades higher than or equal to Grade 4 and less reliable for damage grades lower than Grade 4 (Masi et al. 2017). In order to complement the damage grading maps provided by Copernicus and to provide the possibility of building class identification, the same portfolio of buildings is also subjected to visual survey. The visual survey (Castagna 2017) was based on photography available from field trips (courtesy of G. Forte and A. Santo), videos provided by drone for areas that were difficult to access (Feliziani et al. 2017) and Google Street View. The building by building visual survey is one of the most reliable means for assessing the incurred damage. The portfolio of buildings for which the visual survey is carried out herein is limited by the available photos/ videos. The portfolio of surveyed buildings is limited to residential masonry buildings. However, this is the most widespread structural typology in these towns. Further breaking-down was based on the recommendations in Rota et al. (2008). In Rota et al. (2008), the masonry buildings are classified according to four parameters: 1) number of floors, 2) the presence of tie rods or tie beams, 3) the type of horizontal structure, and 4) regular or irregular masonry layout. However, due to limitation posed by visual survey means, the breaking down into more detailed classifications within the portfolio of residential masonry buildings in this work is limited to two factors: 1) the number of storeys and 2) the presence of tie rods or tie beams. As a result, four distinct classes of masonry buildings have been defined: 1) Masonry buildings without tie rods or tie beams with number of stories ≤2 (Masonry Buildings Class 1, **MBC1**); 2) Masonry buildings without tie rods or tie beams with number of stories >2 (Masonry Buildings Class 2, **MBC2**); 3) Masonry buildings with tie rods or tie beams with number of stories ≤2 (Masonry Buildings Class 3, **MBC3**); 4) Masonry buildings with tie rods or tie beams with number of stories >2 (Masonry Buildings Class 4, **MBC4**). On 13th – 14th September 2016, post-earthquake field recognition identified the valley of Tronto river as the most affected area in terms of site-specific effects. The Tronto valley hosts several municipalities and hamlets. The villages have developed either close to the river (e.g., Trisungo) or on top of the cliffs overlooking it. With the latter being located usually on the top of small ridges and ancient erosional terraces (e.g. Amatrice, Accumoli, Arquata del Tronto) or located on the slopes (e.g. Pescara del Tronto, Illica, Tino). The villages located on cliff-type morphology are bordered by steep slopes (25°-35°) with heights varying from 20 to 80 m. For these areas, buildings labelled with higher levels of damage are widespread and localized near the steep escarpments and in the narrower part of the ridges. These buildings are affected by seismic waves' focalization due to topographic shape effects (e.g., Sanchez-Sesma, 1990; Grelle et al., 2018). These topographic effects are not present in lowland areas of the valley which suffered less damage (see Trisungo). On the other hand, other towns (Amatrice, Pescara del Tronto, Illica and Tino), suffered widespread damage due to both topographic and stratigraphic effects. Some of these towns lie on slopes characterized by few

meters of soft soils resting on a stiffer material (Accumuli); where stiff arenaceous formation of the Laga Flysch is buried by few meters of weathered deposits and colluvium mainly made of silty sands. Pescara del Tronto hamlet lies on debris and travertine sands resting above a limestone bedrock. Vs associated to these deposits are not available and soil classes were based on the lithological association reported in Forte et al., (2017). For instance, D_1 and D_2 are more frequent on stiff rock such as the Arenaceous flysch and limestones; while D_4 and D_5 are more frequent on coarse alluvial deposits, as they are constituted of soft soil.

3.1 *Empirical vulnerability curves*

The vulnerability curves $P(D>D_i|PGA^{16\%})$, $P(D>D_i|PGA^{50\%})$, $P(D>D_i|PGA^{84\%})$, (i=4,5) derived in this study for designated building classes MBC1, MBC2, MBC3, and MBC4 considering the stratigraphic amplification as in options (a) Bindi et al. (2011, grey curves) GMPE and (b) proposed in Landolfi et al. (2011, orange and red curves) are plotted in Figure 1. The observed damage is based on Copernicus EMS database (only damage levels D_4 and D_5 are shown in the figure). The curves corresponding to 16^{th} and 84^{th} percentiles of ground-shaking intensity are plotted as dashed lines and the curves corresponding to the 50^{th} percentile are plotted as solid lines. The comparison shows that the use of stratigraphic coefficients that consider non-linear soil column propagation effects as in Landolfi et al. (2011) is going to lead to a reduction both in median and standard deviation of the vulnerability curves for all the classes. This provides evidence to the fact that consideration of non-linear stratigraphic effects can improve the damage prediction. Figure 2 shows the comparison between the vulnerability curves $P(D>D_i|PGA^{16\%})$, $P(D>D_i|PGA^{50\%})$, $P(D>D_i|PGA^{84\%})$, (i=2,3) obtained based on damage maps of Copernicus EMS (green and yellow curves) and based on the visual survey of damage (grey curves) for MBC1, MBC2, MBC3, and MBC4 (only damage levels D_2 and D_3 are shown in the figure). The comparison demonstrates an overall fine agreement, with the

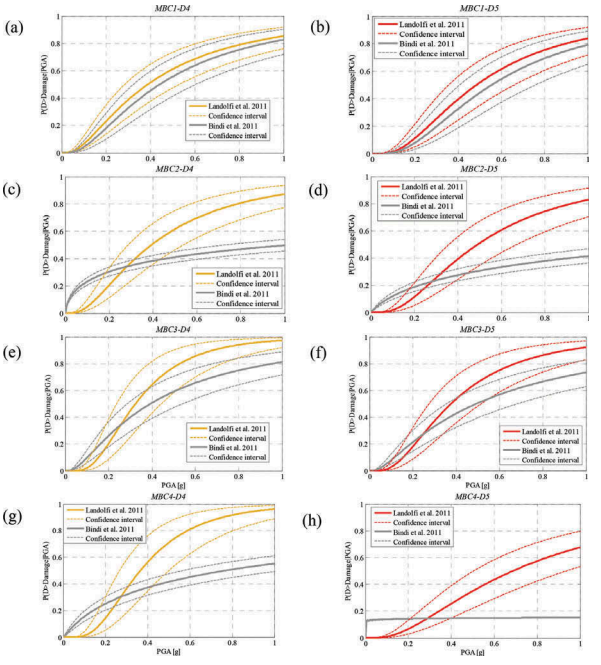

Figure1. Vulnerability curves considering stratigraphic amplification using the coefficients embedded in Bindi et al. (2011) GMPE (option a) and using the factors proposed in Landolfi et al. (2011, option b) for: a) MBC1-D4; b) MBC1-D5; c) MBC2-D4; d) MBC2-D5; e) MBC3-D4; f) MBC3-D5; g) MBC4-D4; h) MBC4-D5.

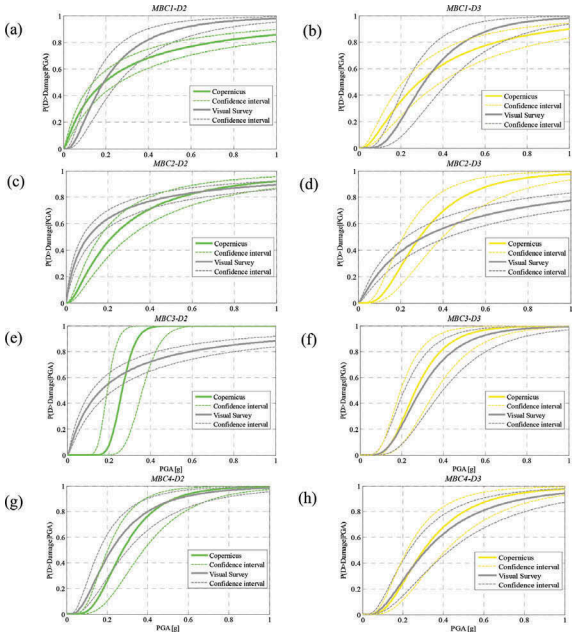

Figure 2. Vulnerability curves considering stratigraphic amplification using the factors proposed in Landolfi et al. (2011, option b) for: a) MBC1-D2; b) MBC1-D3; c) MBC2-D2; d) MBC2-D3; e) MBC3-D2; f) MBC3-D3; g) MBC4-D2; h) MBC4-D3.

exception of a couple of cases. For example, the difference observed between the two sets of curves in the case of $P(D>D_2|PGA^{16\%,50\%,84\%})$ for class MBC3 can be attributed to the small number of buildings (N_{MBC3}=14) in this class. Tables 1 and 2 report equivalent lognormal median and logarithmic standard deviation for the vulnerability curves corresponding to the median ground shaking intensity based on options (a) and (b) with regard to consideration of stratigraphic amplification and based on Copernicus EMS damage grading maps. Table 3 reports the same parameters based on option (b) and with reference to visual damage survey.

Table 1. Equivalent lognormal median and logarithmic standard deviation for vulnerability curves based on median ground shaking intensity which consider stratigraphic amplification as in Landolfi et al. (2011). (damage based on Copernicus EMS).

D2	η [g]	β	D3	η [g]	β	D4	η [g]	β	D5	η [g]	β
MBC1	*0.19*	*1.47*	*MBC1*	*0.29*	*0.93*	*MBC1*	*0.39*	*0.88*	*MBC1*	*0.49*	*0.73*
MBC2	*0.23*	*1.03*	*MBC2*	*0.30*	*0.61*	*MBC2*	*0.40*	*0.81*	*MBC2*	*0.49*	*0.73*
MBC3	*0.26*	*0.18*	*MBC3*	*0.27*	*0.44*	*MBC3*	*0.33*	*0.59*	*MBC3*	*0.38*	*0.71*
MBC4	*0.28*	*0.50*	*MBC4*	*0.31*	*0.77*	*MBC4*	*0.37*	*0.56*	*MBC4*	*0.69*	*0.81*

Table 2. Equivalent lognormal median and logarithmic standard deviation for vulnerability curves based on median ground shaking intensity which consider stratigraphic amplification using coefficients embedded in Bindi et al. (2011) GMPE. (damage based on Copernicus EMS).

D2	η [g]	β	D3	η [g]	β	D4	η [g]	β	D5	η [g]	β
MBC1	*0.19*	*2.08*	*MBC1*	*0.24*	*1.55*	*MBC1*	*0.19*	*2.08*	*MBC1*	*0.24*	*1.55*
MBC2	-	-	*MBC2*	*0.44*	*4.04*	*MBC2*	*1.03*	*3.14*	*MBC2*	*1.68*	*2.38*
MBC3	*0.29*	*0.23*	*MBC3*	*0.21*	*0.88*	*MBC3*	*0.29*	*0.23*	*MBC3*	*0.21*	*0.88*
MBC4	*0.32*	*1.16*	*MBC4*	*0.36*	*3.27*	*MBC4*	*0.77*	*1.99*	*MBC4*	-	-

Table 3. Equivalent lognormal median and logarithmic standard deviation for vulnerability curves based on median ground shaking intensity which consider stratigraphic amplification using coefficients embedded in Landolfi et al. (2011). (Visual damage survey).

D2	η [g]	β	D3	η [g]	β	D4	η [g]	β	D5	η [g]	β
MBC1	*0.19*	*0.80*	*MBC1*	*0.32*	*0.55*	*MBC1*	*0.38*	*0.60*	*MBC1*	*0.63*	*0.90*
MBC2	*0.11*	*1.72*	*MBC2*	*0.31*	*1.49*	*MBC2*	*0.42*	*0.87*	*MBC2*	*0.86*	*1.26*
MBC3	*0.16*	*1.64*	*MBC3*	*0.29*	*0.51*	*MBC3*	*0.29*	*0.51*	*MBC3*	*0.49*	*0.61*
MBC4	*0.22*	*0.70*	*MBC4*	*0.32*	*0.72*	*MBC4*	*0.36*	*0.54*	*MBC4*	*0.49*	*0.65*

4 CONCLUSIONS

Empirical vulnerability curves for masonry buildings based on 16th, 50th and 84th percentiles of ground-shaking intensity (in PGA terms) have been derived. The ground-shaking fields are generated by updating the GMPE-based values by employing registered accelerometric data. The observed damage data for masonry buildings are collected in the aftermath of the 2016 Amatrice Earthquake. Ground shaking propagated to the bed rock level using the GMPE has been modified based on site-specific stratigraphic and topographic effects. Using the soil stratigraphic factors proposed in Landolfi et al. (2011), which consider non-linear soil column effects, helps in reducing the dispersion in the vulnerability curves. An overall acceptable agreement is observed between vulnerability curves obtained based on Copernicus EMS and visual survey. This gives credit to large-scale damage survey by means of remote sensing.

ACKNOWLEDGMENTS

This work is based on visual damage survey results described in the B.Sc. thesis of Filomena Castagna. This support is gratefully acknowledged.

REFERENCES

Baker, J.W. 2015. Efficient analytical fragility function fitting using dynamic structural analysis. *Earthquake1 Spectra* 31(1), 579–599.

Bindi D., Pacor F., Luzi L.,. . ., Paolucci R. 2011. Ground motion prediction equations derived from the Italian strong motion database. *Bulletin of Earthquake Engineering* 9(6):1899–1920

Castagna, F. 2017. La valutazione della vulnerabilità sismica degli edifici danneggiati a seguito del terremoto di Amatrice del 24 agosto 2016. B.Sc. in civil engineering, university of Naples Federico II.

Charvet, I., Ioannou, I., Rossetto, T., Suppasri, A., Imamura, F. 2014. Empirical fragility assessment of buildings affected by the 2011 Great East Japan tsunami using improved statistical models. *Natural Hazards* 73(2), 951–973.

Crowley H, Bommer JJ, Stafford PJ (2008) Recent developments in the treatment of ground-motion variability in earthquake loss models. J Earthq Eng 12(S2):71–80

De Luca, F., Verderame, G.M., Manfredi, G. 2015. Analytical versus observational fragilities: the case of Pettino (L'Aquila) damage data database. *Bulletin of Earthquake Engineering* 13(4):1161–1181.

Del Gaudio, C., De Martino, G., Di Ludovico, M., Manfredi, G., Prota, A., Ricci, P., Verderame, G. M. 2017. Empirical fragility curves from damage data on RC buildings after the 2009 L'Aquila earthquake. *Bulletin of Earthquake Engineering* 15(4), 1425–1450.

De Risi, R., Jalayer, F., De Paola, F., Lindley, S. 2017. Delineation of flooding risk hotspots based on digital elevation model, calculated and historical flooding extents: the case of Ouagadougou. *Stochastic Environmental Research and Risk Assessment* 1–15.

Dolce, M., Goretti, A. 2015. Building damage assessment after the 2009 Abruzzi earthquake. *Bulletin of Earthquake Engineering* 13(8), 2241–2264.

Ebrahimian, H., Jalayer, F. 2017. Robust seismicity forecasting based on Bayesian parameter estimation for epidemiological spatio-temporal aftershock clustering models. *Scientific reports* 7(1), 9803.

Esposito, S., Iervolino, I. 2012. Spatial correlation of spectral acceleration in European data. *Bulletin of Seismological Society of America* 102(6):2781–2788

Feliziani. F.,. . ., Fiorini. M., 2017. 2D and 3D models in emergency scenarios: UAVs for planning search and rescue operations and for preliminary assessment of high buildings. *Proc of UAVandSAR2017*-International workshop-Rome.

Forte, G., Fabbrocino, S., Fabbrocino, G., Lanzano, G., Santucci de Magistris, F., Silvestri F. 2017. A geolithological approach to seismic site classification: an application to the Molise Region (Italy). *Bulletin of Earthquake Engineering* 15 (1), 175–198.

Grelle, G., Bonito, L., Maresca, R., Maufroy, E., Revellino, P., Sappa, G., Guadagno, F. 2018. Topographic effects in Amatrice suggested from the SISERHMAP predictive model, seismic data and damage. *Proceedings-16th european conference on earthquake engineering*, Thessaloniki, June 2018.

Grünthal, G. 1998. Cahiers du Centre Europe´en de Ge´odynamique et de Se´ismologie: vol. 15-European Macroseismic Scale. *European Center for Geodynamics and Seismology*, Luxembourg.

Jalayer, F., Ebrahimian, H. 2017. Seismic risk assessment considering cumulative damage due to aftershocks. *Earthquake Engineering and Structural Dynamics* 46(3), 369–389.

Jalayer, F., Ebrahimian, H., Miano, A., Manfredi, G., Sezen, H. 2017. Analytical fragility assessment using un-scaled ground motion records. *Earthquake Engineering and Structural Dynamic* 46(15), 2639–2663.

Lagomarsino, G., Giovinazzi, S. 2006. Macroseismic and mechanical models for the vulnerability and damage assessment of current buildings. *Bulletin of Earthquake Engineering* 4:415–443.

Lallemant, D., Kiremidjian, A., Burton, H. Statistical procedures for developing earthquake damage fragility curves. *Earthquake Engineering & Structural Dynamics* 44.9 (2015): 1373–1389.

Landolfi, L., Caccavale, M., d'Onofrio, A., Silvestri, F., Tropeano G. 2011. Preliminary assessment of site stratigraphic amplification for Shakemap processing. *Proceedings of V ICEGE, Santiago*, p.5.3.

Masi, A., Chiauzzi, L., Santarsiero, G., Liuzzi, M., Tramutoli, V. 2017. Seismic damage recognition based on field survey and remote sensing: general remarks and examples from the 2016 Central Italy earthquake. *Natural Hazards* 86(1), 193–195.

Miano, A., Jalayer, F., De Risi, R., Prota, A., Manfredi, G. 2015. A case-study on scenario-based probabilistic seismic loss assessment for a portfolio of bridges. *Proc. of 12th international conference on applications of statistics and probability in civil engineering*, Vancouver, Canada, July, 2015.

Miano, A., Jalayer, F., De Risi, R., Prota, A., Manfredi, G. 2016. Model updating and seismic loss assessment for a portfolio of bridges. *Bulletin of Earthquake Engineering* 14(3), 699–719.

Miano, A., Jalayer, F., Ebrahimian, H., Prota, A. 2018. Cloud to IDA: Efficient fragility assessment with limited scaling. *Earthquake Engineering and Structural Dynamics* 47(5), 1124–1147.

Park, J., Bazzurro, P., Baker, J.W. 2007. Modeling spatial correlation of ground motion intensity measures for regional seismic hazard and portfolio loss estimation. *Applications of statistics and probability in civil engineering*. Taylor & Francis Group, London, pp 1–8.

Rossetto, T., Elnashai, A. 2003. Derivation of vulnerability functions for European-type RC structures based on observational data. *Engineering structures* 25(10), 1241–1263.

Rota, M., Penna, A., Strobbia, C.L. 2008. Processing Italian damage data to derive typological fragility curves. *Soil Dynamics and Earthquake Engineering* 28(10):933–947

Silvestri, F., Forte, G., Calvello, M. 2016. Multi-level approach for zonation of seismic slope stability: Experiences and perspectives in Italy. *Landslides and Engineered Slopes. Experience, Theory and Practice*–Aversa et al. (Eds), Associazione Geotecnica Italiana, Rome, Italy.

Sanchez-Sesma, F.J. 1990. Elementary solutions for response of a wedge-shaped medium to incident SH and SV waves. *Bulletin of Seismological Society of America* 80: 737–742.

Singhal, A., Kiremidjian, A.S. 1998. Bayesian updating of fragilities with application to RC frames. *Journal of Structural Engineering* 124(8):922–929.

Torgoev,A., Havenith, H.B., Lamair, L. 2013. Improvement of seismic landslide susceptibility assessment through consideration of geological and topographic amplification factors. *JAG,Grenoble, France*.

Tropeano, G., Soccodato, F.M., Silvestri, F. 2018. Re-evaluation of code-specified stratigraphic amplification factors based on Italian experimental records and numerical seismic response analyses. *Soil Dynamics and Earthquake Engineering* 110, 262–275

Zuccaro, G., Cacace, F. 2015. Seismic vulnerability assessment based on typological characteristics. The first level procedure "SAVE". *Soil Dynamics and Earthquake Engineering* 69:262–269.